JOURNAL OF GEOPHYSICAL RESEARCH, VOL. 105, NO. D8, PAGES 10,147–10,160, APRIL 27, 2000

Extended range forecasts over South America using the regional eta model

S. C. Chou, A. M. B. Nunes, and I. F. A. Cavalcanti

Centro de Previsão de Tempo e Estudos Climáticos (CPTEC), Instituto Nacional de Pesquisas Espaciais (INPE), Cachoeira Paulista, Brazil

Abstract. An 80-km National Centers for Environmental Prediction eta model was configured to run over the South America continent. This limited area model has 38 layers in the atmosphere, and its domain includes part of the adjacent Atlantic and Pacific Oceans. The model was setup to perform 1 month forecasts. The version used in these preliminary experiments uses a bucket model to describe water in the ground and a modified Betts-Miller scheme for producing convective precipitation. The experiments used constant sea surface temperature field and initial soil moisture from climatology. Results obtained from a dry season month and a rainy season month over South America in 1997 show that the reinitialization of model at short range forecasts is not necessary as was done with the previous version of the model. These results show no obvious drying of the atmosphere or tendency with time of the domain average surface pressure. In both cases (dry and wet) the model seems to have reproduced the climatological signal of the forecast months. The monthly accumulated total precipitation agrees well with the observations. These runs showed that the current configuration of the eta model is stable and capable of producing continuous extended range runs over South America.

1. Introduction

Climate prediction has been improving through the use of coupled ocean-atmosphere models (coupled general circulation model (CGCM)) which contain the interaction between sea surface temperature (SST) and the atmosphere, thus preventing the use of constant SST anomalies or predicted SST in global atmospheric models. The horizontal and vertical resolutions of an atmospheric general circulation model (AGCM) are also important to provide good forecasts, as shown in a numeric experiment carried out by *Cavalcanti et al.* [1995].

The present limitation of resolution for AGCMs and CGCMs, which are partly dependent on the computer capability to simulate small-scale features of meteorological variables, makes the regional models particularly attractive in climate prediction. Often, small to synoptic features contribute to the precipitation field which are not detected in GCMs and the prediction of precipitation lead only by large-scale features end up in erroneous predictions.

A limited area model can have higher resolution and resolve the orography better than GCMs. For South America the model response to synoptic systems is crucial, particularly for the south and southeast regions which are affected frequently by extratropical cyclones and anticyclones passages. In the tropics, the CPTEC/COLA (Centro de Previsão de Tempo e Estudos Climáticos / Center for Ocean-Land-Atmosphere Studies) global model forecasts frequently capture the large-scale easterly disturbances that affect the northern and northeastern part of Brazil; however, smaller-scale organized convections, which are generally embedded in these disturbances and can produce large amounts of precipitation, are better forecast by the regional eta model [*Bonatti et al.*, 1996; *Souza et al.*, 1998].

The first attempt to produce a more detailed description of the climate over a region was done by nesting the 60-km National Center for Atmospheric Research (NCAR) - Pennsylvania State University mesoscale model (MM4) into the NCAR GCM [*Dickinson et al.*, 1989]. In this work the GCM, with rhomboidal truncation R15, predicted unrealistic precipitation over the western United States; nevertheless, the higher-resolution model corrected the precipitation forecast.

The NCAR regional model with 50-km resolution has been used to simulate the summertime monsoon circulation over east Asia [*Giorgi et al.*, 1993; *Liu et al.*, 1994]. The simulation captured the sudden movement of the rain belt during the establishment of the monsoon system. The wet centers of soil moisture were also captured by the simulations. These detailed features had

Paper number 1999JD901137.
0148-0227/00/1999JD901137$09.00

major contribution from the high-resolution vegetation and topography of the regional model.

Tanajura [1996] and *Ji and Vernekar* [1997] used the regional eta model to describe the continental climate circulations. The former described the typical summer circulation over South America by capturing the South Atlantic Convergence Zone (SACZ) and the Bolivian High systems. The latter described the Indian summer monsoon. In both runs the model used 80-km horizontal resolution, was restarted at every 48 hours of integration, and used a previous version of the model.

A successful attempt to perform a continuous extended range run with the eta model was carried out by *Dacić* [1997]. The model was setup with a 60-km horizontal resolution and produced a 26-day simulation of the circulation over the Mediterranean region. The model exhibited stability through the integration period. The simulated fields were comparable to the analysis fields which proved the model is capable of producing continuous longer-term runs.

The objective of this work is to perform and evaluate extended range forecasts with the regional eta model and, ultimately, to develop a tool for climate prediction over South America. In this preliminary study, the regional eta model was used to produce 1-month forecasts over South America for two contrasting precipitation regime months, a wet and a dry. In section 2 a brief description of the model is given. The configuration of the experiments is described in section 2.3. Model stability is presented in section 3. Verification of the forecasts is done in section 4. Finally, discussions and conclusions are drawn in section 5.

2. Methodology

2.1. Eta model

The model was configured with 80-km resolution and 38 layers in the vertical. The domain covers most of South America, from ~ 13°N up to ~ 50°S and part of the adjacent oceans. The prognostic variables are temperature, specific humidity, winds, surface pressure, turbulent kinetic energy, and cloud water. The equations are solved on the E grid and integrated through a split-explicit scheme based on the forward-backward and the Euler-backward schemes, both modified by *Janjić* [1979]. The finite space difference uses the Janjić method [*Janjić,* 1984].

One of the features of this model is the vertical coordinate, η, defined as [*Mesinger,* 1984]

$$\eta = \frac{p - p_t}{p_s - p_t}\frac{p_r(z) - p_t}{p_r(0) - p_t}, \quad (1)$$

where p is the pressure, subscripts s, t, and r, refer to the surface, the top of the atmosphere, and a reference state, respectively, and z is the height. This coordinate is also known as a step-mountain coordinate, as the top of the mountains coincide with the model interfaces forming steps. The η surfaces are practically horizontal. This feature reduces the problems related to errors found in the commonly used σ vertical coordinate which are caused by calculations of horizontal derivatives. A drawback of the η coordinate is the decrease in the vertical resolution at higher layers which results in poorly resolved boundary layers at elevated hills. Figure 1 shows the 80-km resolution steps that form the South America orography used by the model.

The cumulus convection parameterization uses a modified Betts-Miller scheme [*Betts and Miller,* 1986; *Janjić,* 1990; 1994]; turbulence is represented by Mellor-Yamada 2.5 scheme in the free atmosphere and Mellor-Yamada 2.0 in the surface layer [*Mellor and Yamada,* 1974]. Further details on the model are given by *Black* [1994]. In the context of this work, a relevant feature of this version of the model is the treatment of soil water by the Bucket scheme [*Manabe,* 1969]. The model bucket capacity is 150 mm. The surface temperature results from the surface heat balance, and soil water results from a balance between precipitation and evaporation and is limited to 75% of the bucket capacity, the excess is lost as runoff. Evaporation occurs at a fraction β of potential evaporation, where β is the ratio between soil water content and soil water content at field capacity.

2.2. Global Model

The GCM used in this study is the CPTEC/COLA GCM, which is a model implemented by the Center for Ocean-Land-Atmosphere Studies and derived from the NCEP model [*Kinter et al.,* 1988]. This model is used at CPTEC for weather forecasts and also for seasonal prediction; it is a global spectral model with horizontal triangular resolution, T62, and 28 levels in σ coordinate. The primitive equations and the physical processes are described by *Kinter et al.* [1997]. The version used in this experiment applies the Kuo scheme [*Kuo,* 1974] for deep convection, and the shallow convection is parameterized following *Tiedtke* [1983]. The Mellor-Yamada closure scheme is applied for the vertical diffusion [*Mellor and Yamada,* 1982], and a biharmonic type diffusion is used for the horizontal diffusion. The shortwave radiation is that of *Lacis and Hansen* [1974], modified by *Davies* [1982], and the longwave heating formulation was developed by *Harshvardhan et al.* [1987]. The model includes a sophisticated biosphere scheme [*Xue et al.,* 1991], which is important for climate forecast over a continent covered by a significant portion of tropical rain forest.

2.3. Experiments Description

Two extended runs were performed: one for a dry month in the central and southeast regions, August 1997, and another for a rainy month in those regions, November 1997, which is spring in the Southern Hemisphere and the rainy period is resuming over South

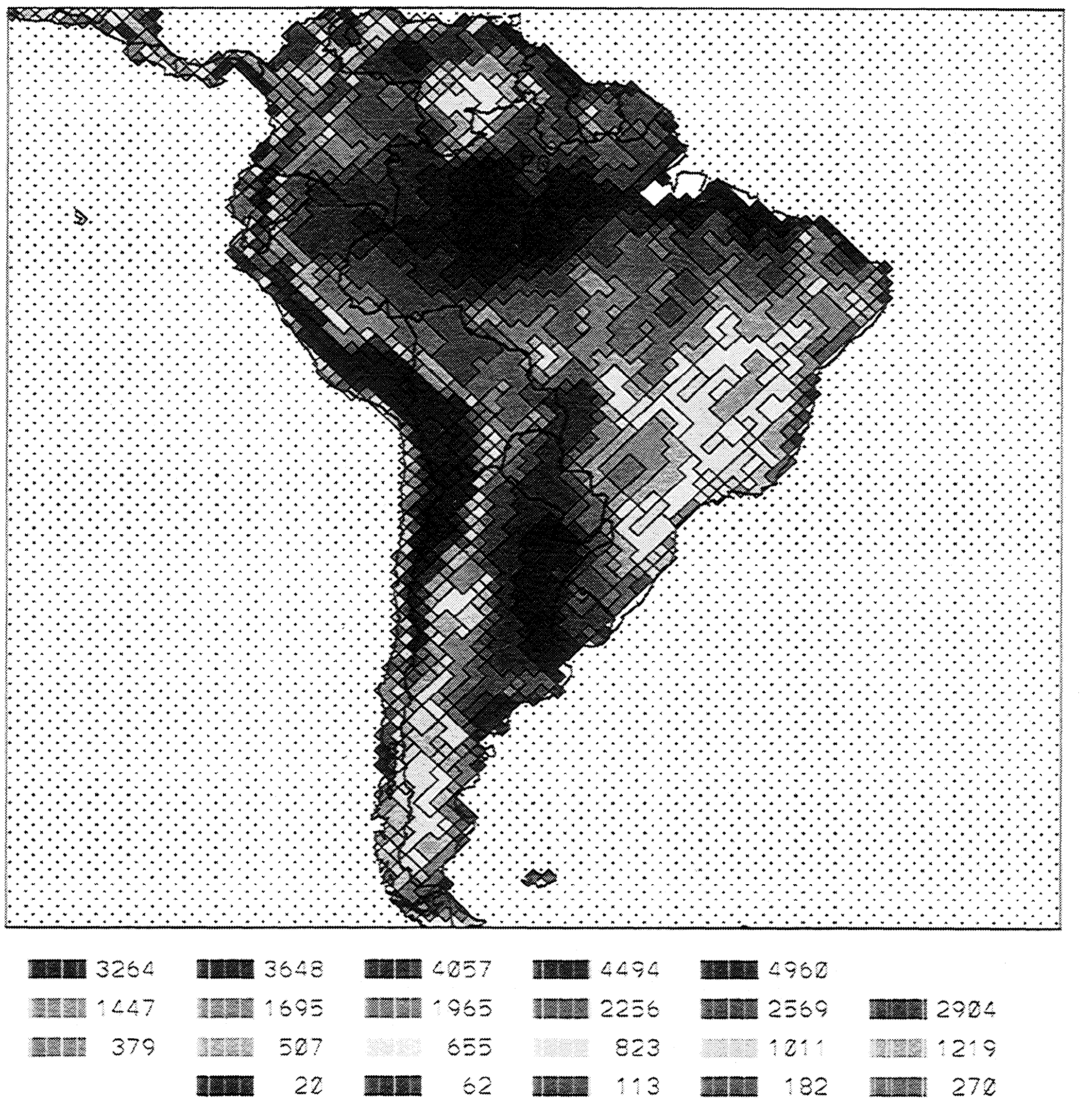

Figure 1. South America 80-km eta model topography.

America. The model was integrated from 1200 UTC August 1, 1997, and from 0000 UTC November 1, 1997, using NCEP analyses as initial conditions. Forecasts from CPTEC/COLA GCM were taken as lateral boundary conditions, which were updated every 6 hours and the tendencies distributed linearly within this time interval. Initial lower boundary conditions used annual climatology of soil moisture, and sea surface temperature was taken from the weekly mean observations on the day 1 of the forecast and kept constant during the 1-month integrations. Albedo was taken from seasonal climatology.

The regional eta model performed continuous 30-day integrations, without being restarted at short forecasts. The continuous run allows the model to develop its own climate with reduced influence from the initial conditions, which were originated from a coarser and different physics model. The technique of performing extended run with the regional model is also employed for testing purposes whenever implementations are introduced to the model [*Sass and Christensen*, 1995].

Long-term integrations are evaluated by taking the sign and intensity of the model anomalies and comparing with observed anomalies. This methodology excludes model systematic bias or the model climatological deviation from the forcing fields, as defined by *Giorgi and Mearns* [1999], and can improve skill of the results. However, eta model climatology from long-term integrations over South America is not yet available to allow computation of the anomalies. In this study, verification is performed with the full fields instead of anomalies.

3. Model Stability

Model stability for long-term integration was assessed in *Dacić* [1997] version of the eta model, based on nor-

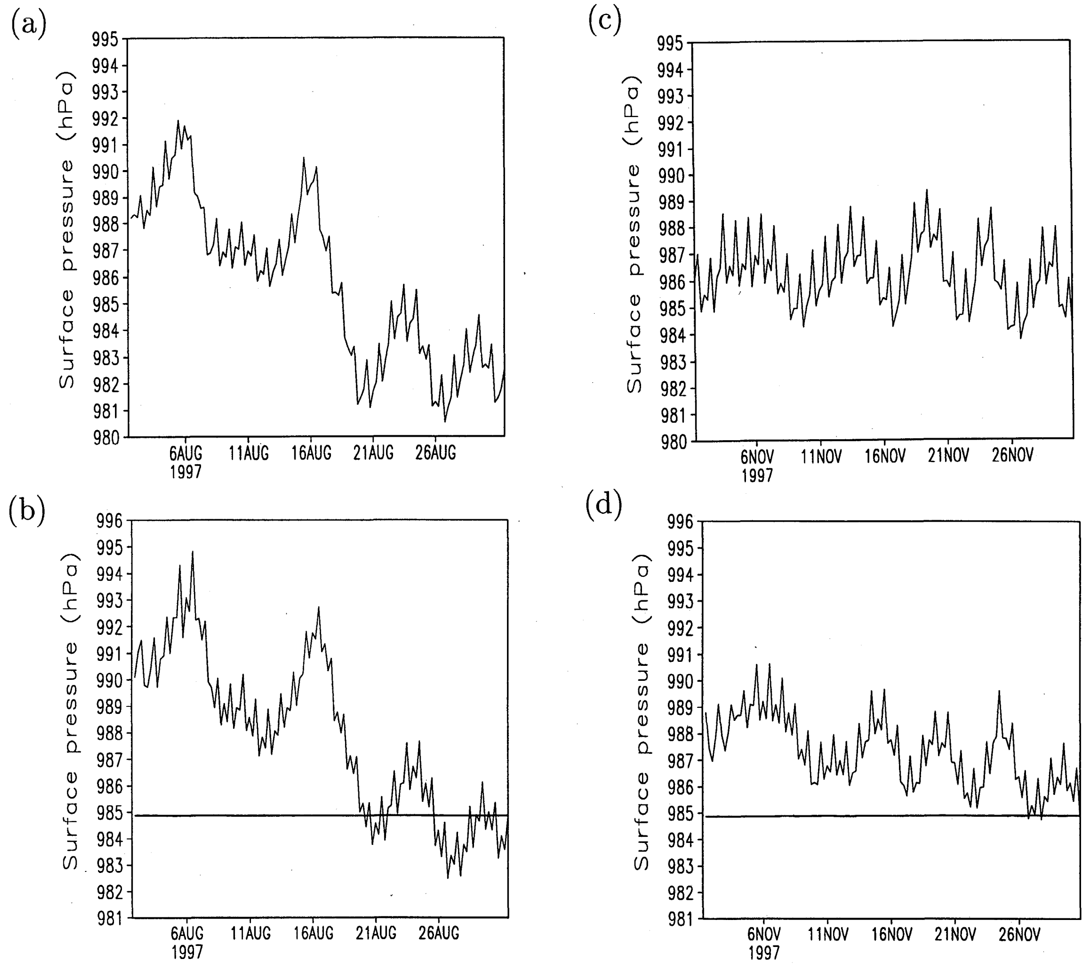

Figure 2. Surface pressure (hPa) averaged over the regional domain, predicted for August 1997 by (a) eta model and (b) global model and predicted for November 1997 by (c) eta model and (d) global model. Thin solid lines refer to average taken over the South America region: 50°S, 10°N and 26°W, 90°W. Thick solid lines in Figures 2b and 2d refer to average over global domain, indicating model conservation of air mass.

malized energy. Here, the model stability is further assessed based on the mass conservation. The stability in a limited area model can be tricky. The conservation of the properties may be affected in different ways. The penetration of a frontal system into the domain may result in a sudden decline of the temperature and surface pressure, if the domain is small this decline can be very sharp. The assessment of the model stability can be also largely affected if done during the transition of seasons. Finally, the length of the forecast is another important aspect to be considered; there should be a compromise between the size of the model errors and the length of useful forecast.

Figure 2a shows the regional domain average surface pressure through the integration period for the dry month. A sudden decrease in surface pressure occurs on day 16 and assumes a lower value for the rest of the integration. This decrease could suggest a mass loss by the model; however, the average of surface pressure from the global model, taken over the same regional domain (Figure 2b) shows the same decreasing tendency. The globally averaged surface pressure is constant during the whole integration period, which indicates the mass conservation by the global model. The sudden decrease of the mean surface pressure was caused by the passage of an intense low-pressure system across the domain. This decrease did not occur in the rainy month (Figures 2c and 2d).

To show that there is no evident systematic dry-out through the model integration, atmospheric volume average of specific humidity was computed over the regional model domain. Figure 3a shows a sharp decrease in the mean specific humidity on day 9; an increase occurs after day 11 and recovers the original magnitude. The same domain average of specific humidity taken from the global model (Figure 3b) shows similar tendency on day 9, although the decrease is not as sharp as in the regional model. The tendency of specific humidity from the regional model follows closely the global model tendency, however, at different magnitudes. The

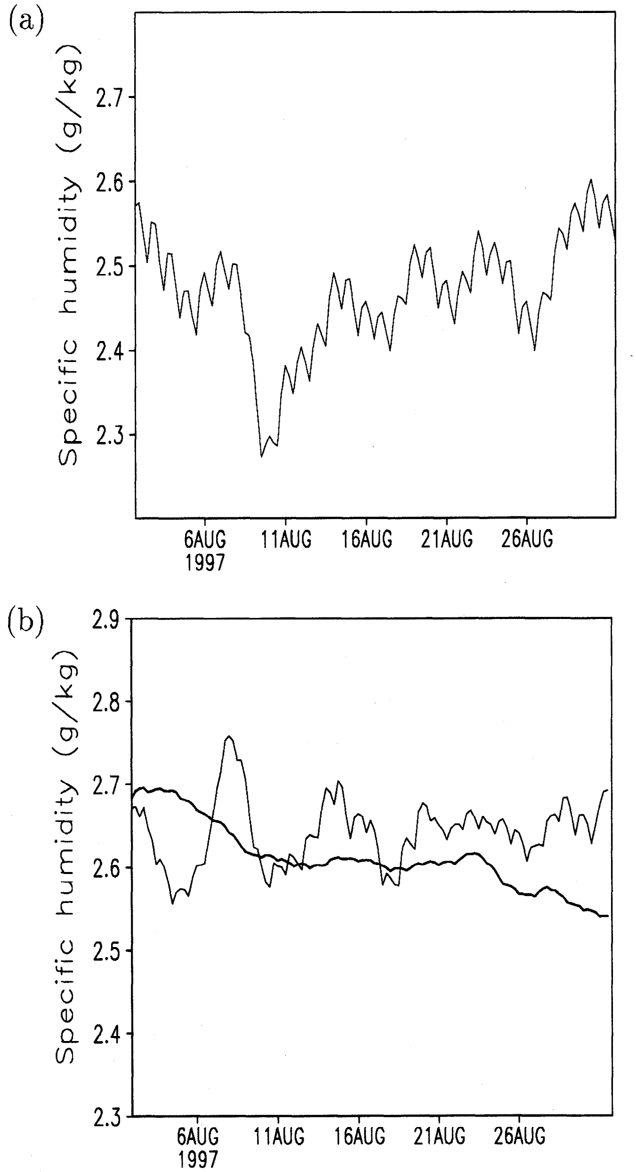

Figure 3. Specific humidity ($g\,kg^{-1}$) averaged over the regional domain, predicted for August 1997 by (a) eta model and (b) global model. Thick solid line in Figure 3b refers to average over global domain.

global model contains more moisture in the atmosphere.

Owing to the high precision and accuracy needed in the computation of moisture related variables and the different treatment in the numerical models, moisture fields show large differences from one model to another. The precipitation production is a major mechanism that changes moisture field. The global model employs the Kuo scheme [*Kuo,* 1974] to treat the convective precipitation, while the regional model uses the modified Betts-Miller scheme. The soil water also receives very distinct treatment by both models.

Curves of the time series of average precipitation from the regional model follow very closely the equivalent curves from the global model runs Figure 4. This suggests that the large-scale variability of precipitation was kept in the regional model. The global model produced larger amounts of precipitation. No evident dry-out can be noticed from the precipitation or moisture fields.

The domain average of the variables for the wet case showed better agreement between the regional and the global model forecast tendencies than the dry case. These domain averaged fields showed that the model was well configured and conserving the necessary properties for stability which indicates the model suitability for extended range integrations.

4. Forecast Verifications

The verification of model output is an important step previous to its use for description of atmospheric conditions. The skill of regional climate model has been carried out for the MM4 version over the western United States [*Giorgi and Bates,* 1989]. Here model verification

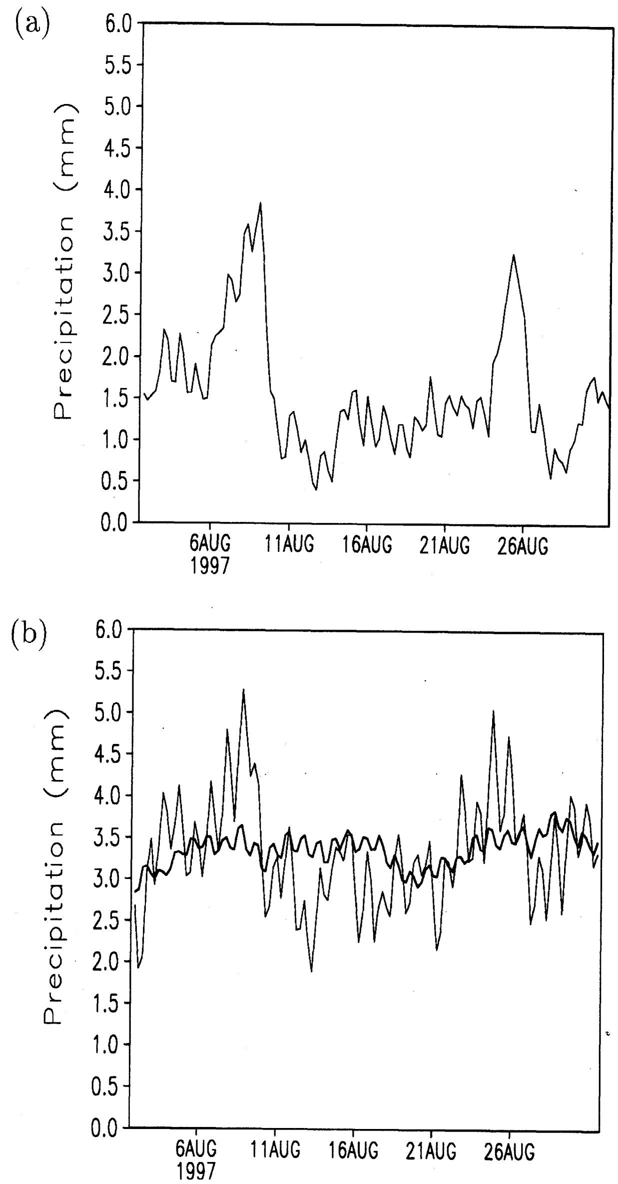

Figure 4. Total precipitation (millimeter) averaged over the regional domain, predicted for August 1997 by (a) eta model and (b) global model. Thick solid line in Figure 4b refers to average over global domain.

is based on the monthly total precipitation, surface temperature, outgoing longwave radiation (OLR), and the equitable threat score for both dry and wet months. A three-way comparison is carried out with the observations, regional model, and global model.

Monthly total precipitation and mean temperature observed data were provided by the Brazilian Meteorological Institute (INMET). These data are based on a total of ~ 250 surface observations over the Brazilian territory only. INMET computes the mean temperature based on the formula: $((2)T00Z + T_{\max} + T_{\min} + T12Z)/5$, where $T00Z$ and $T12Z$ are shelter temperatures at 0000 and 1200 UTC, respectively, and $T_{\max}$ and $T_{\min}$ are the maximum and minimum temperatures of the day, respectively.

An interpolated OLR data set [*Liebmann and Smith,* 1996] was obtained from twice daily advanced very high resolution radiometer (AVHRR) soundings from the National Oceanic and Atmospheric Administration (NOAA) polar-orbiting satellite, with equatorial crossing times at 0230 and 1430 LST (Local Standard Time) (NOAA 14), and averaged for the month. For the studied period, however, the data were constructed from one daily passage at 1430 LST. Because of differences between model and observation variables, forecast verification will be based mostly on the patterns; therefore the figures were plotted on the same domain and used the same contours.

Equitable threat score (ETS) can be calculated by the expression [e.g., *Mesinger and Black,* 1992]:

$$\mathrm{ETS} = \frac{H - CH}{F + O - H - CH} \qquad (2)$$

where $CH = (FO)/N$, F is the number of forecast precipitation events above a certain threshold, O is the number of observed events above the threshold, H is the number of hits, and N is the number of grid-points. The bias score is defined as: $\mathrm{BIAS} = F/O$. ETS and BIAS scores are used together, and a perfect forecast is equivalent to ETS = 1 and BIAS = 1. The amounts of precipitation were divided into 8 categories: 9, 30, 50, 100, 200, 300, 400, and 600 mm. Precipitation forecasts have been evaluated for short-term 1997 forecasts by *Chou and Justi da Silva* [1999]. Here the evaluation is based on a monthly total which results in higher scores as the timing of the daily precipitation event is not taken into account. The observed and the regional model monthly total precipitation fields were interpolated, by the kriging and linear methods, respectively, onto the global model output grid of 1.875° × 1.875° latitude-longitude resolutions. The score was computed on every grid box which contained at least one observation.

4.1. Dry Month Run: August 1997

4.1.1. Precipitation. The central part of the country was dry, and no precipitation occurred during this month as shown in Figure 5a. The no-precipitation

(a) (b) (c)

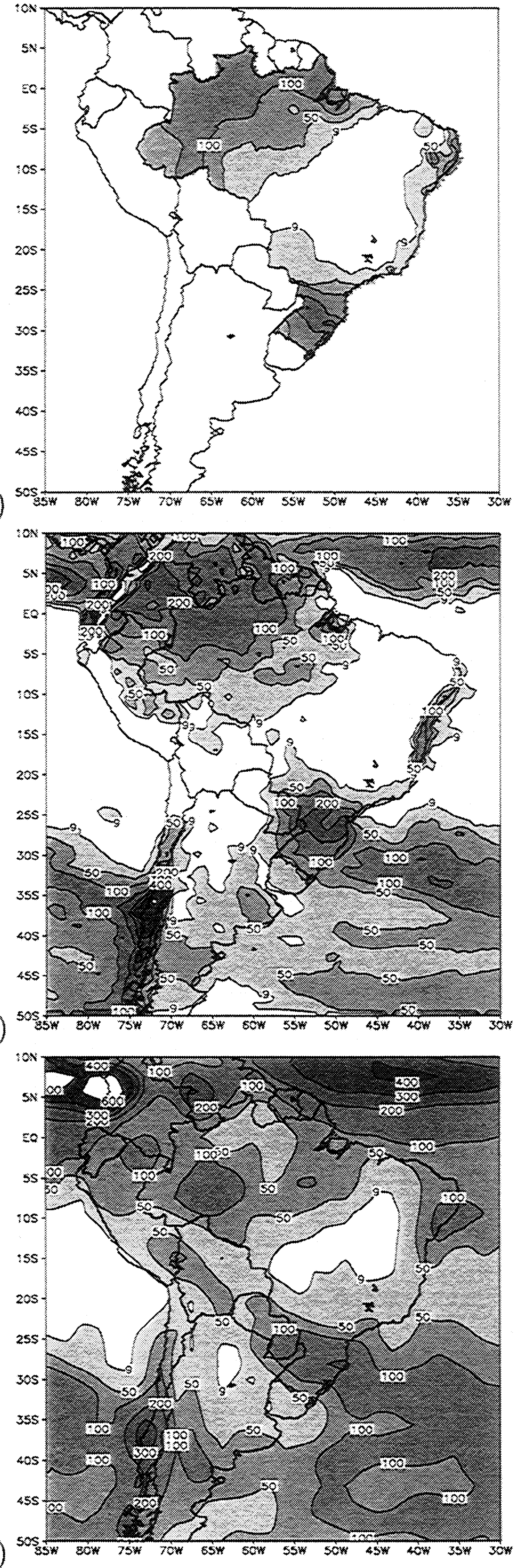

Figure 5. August 1997 total precipitation (millimeter): (a) observed over Brazil, (b) the regional eta model forecast, and (c) the global model forecast.

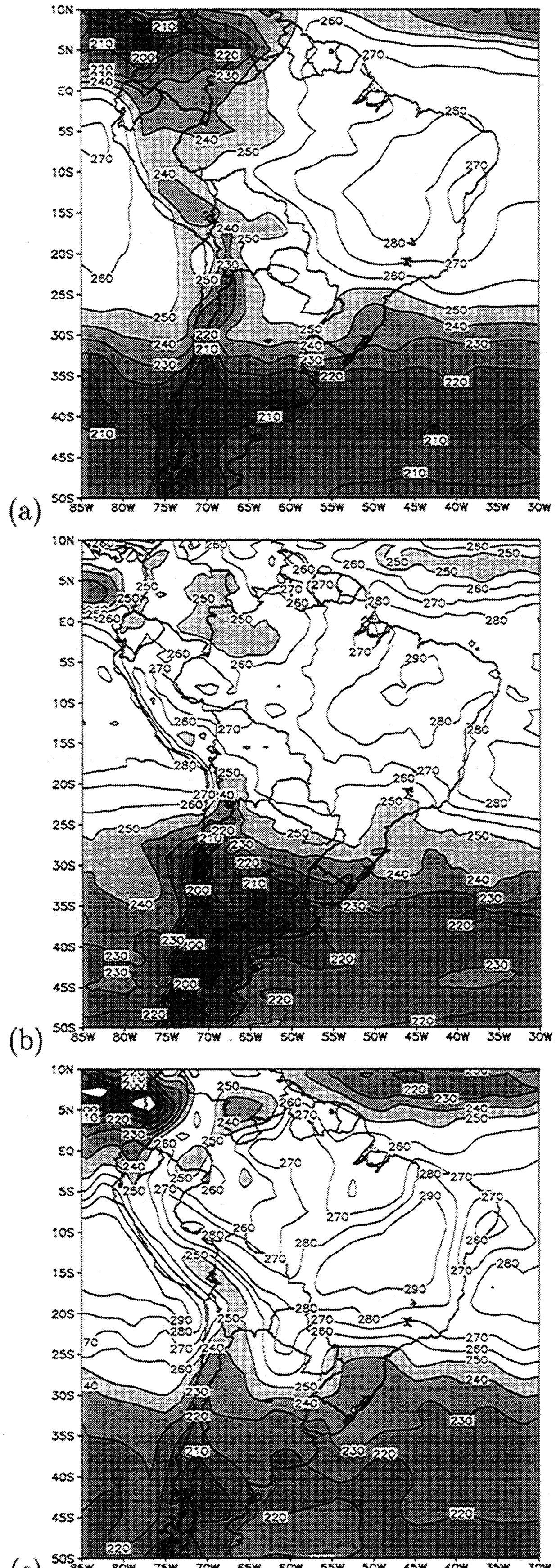

Figure 6. Outgoing longwave radiation $\mathrm{Wm^{-2}}$, average of August 1997. (a) Mean OLR. (Data provided by the NOAA-CIRES Climate Diagnostics Center, Boulder, Colorado, available at http://www.cdc.noaa.gov/.) (b) Regional eta model forecast, and (c) global model forecast.

borderline was well captured by the regional model (Figure 5b); however, it was overdried in some parts of northeast Brazil, mainly in the northeastern coast. In the Amazon region and also in the South, where precipitation occurred regularly, the model prediction closely follows the observed amounts. Although little precipitation was reported by INMET along the coast of Bahia, automatic surface weather stations reported total precipitation of the order of 100 mm, which was closer to the predicted values.

A comparison with the precipitation amounts produced by the global model showed that the regional model can create a climate of its own. The general pattern of the precipitation contours from the GCM forecasts (Figure 5c) is also similar to the observations; however, the no-precipitation regions are small. Precipitation over south and northeast Brazil are reasonably captured by the GCM model. The regional model precipitation forecasts for Argentina and Chile show good agreement with the daily accumulated precipitation observed from automatic surface stations. During August 1997, floods were reported to occur in Chile. The GCM forecast showed values over 300 mm on the central Chile, whereas the regional model produced precipitation over 500 mm. *Bell and Halpert* [1998] stated that the precipitation in Santiago, Chile, from August to October 1997 reached 300% of the normal for the period.

4.1.2. OLR. The largest values of observed OLR during this dry month, $\sim 280\,\mathrm{W\,m^{-2}}$, are probably associated with generally cloud free areas, which were observed over central and northeastern parts of Brazil (Figure 6a). These cloud free regions are supported by observations of precipitation (Figure 5a). The regional model predicted OLR values (Figure 6b) higher than the observations and with the maximum values expanding westwards in the tropics. In the middle latitudes over the Andes, the regional model predicted smaller OLR. However, the general pattern of OLR showed good agreement with observations. The global model forecast of OLR (Figure 6c) exhibited a wider area within the $280\,\mathrm{W\,m^{-2}}$ which extended farther westward than the regional model. OLR was overestimated by both models in the region of the study.

4.1.3. Temperature. Figure 7a shows the August mean observed shelter temperature which can be compared with the predicted mean surface temperatures by the regional model (Figure 7b) and by the global model (Figure 7c). In this verification the pattern similarity of the temperature fields is the parameter for the comparison as the variables are computed differently.

The penetration of cold air from South and along the eastern coast is predicted in both models; however, a larger degree of detail is provided by the regional model. The isotherm of 22°C for example, which reaches the south part of northeast Brazil, is only captured by the regional model. A major factor to control the mean temperature near the surface is the topography. The regional model has the advantage of higher resolution and better representation of the topography than the

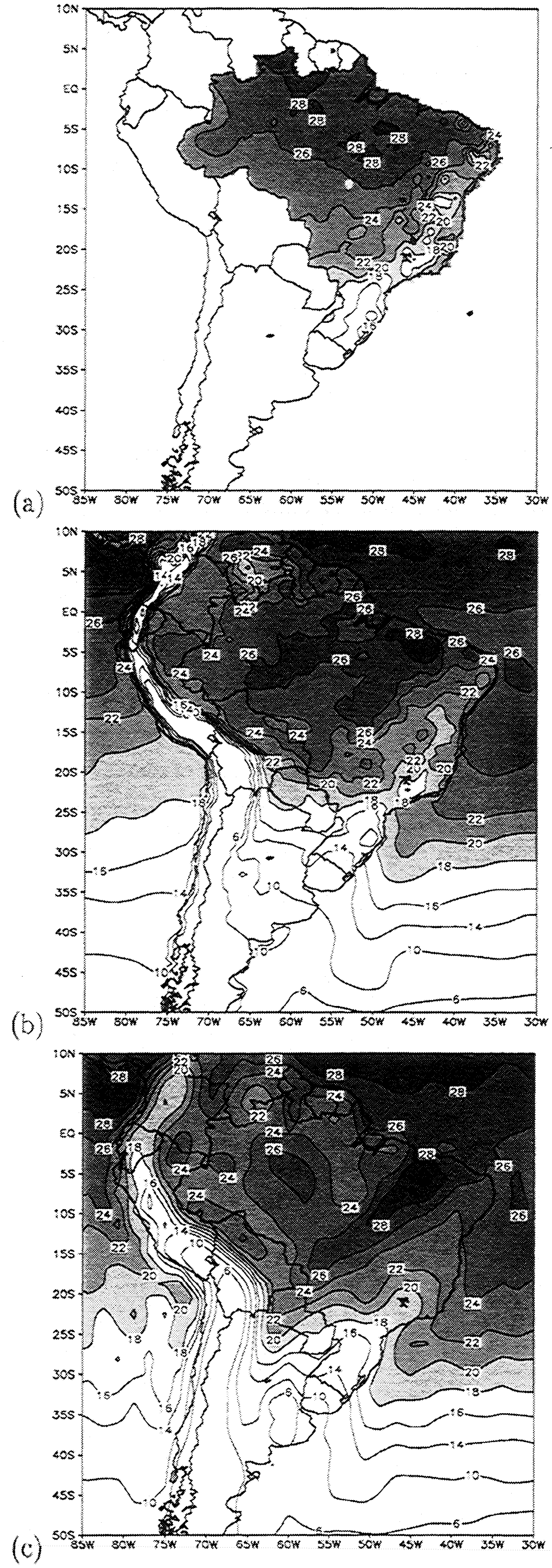

Figure 7. August 1997 Surface temperature (K): (a) observed, (b) regional eta model forecast, and (c) global model forecast.

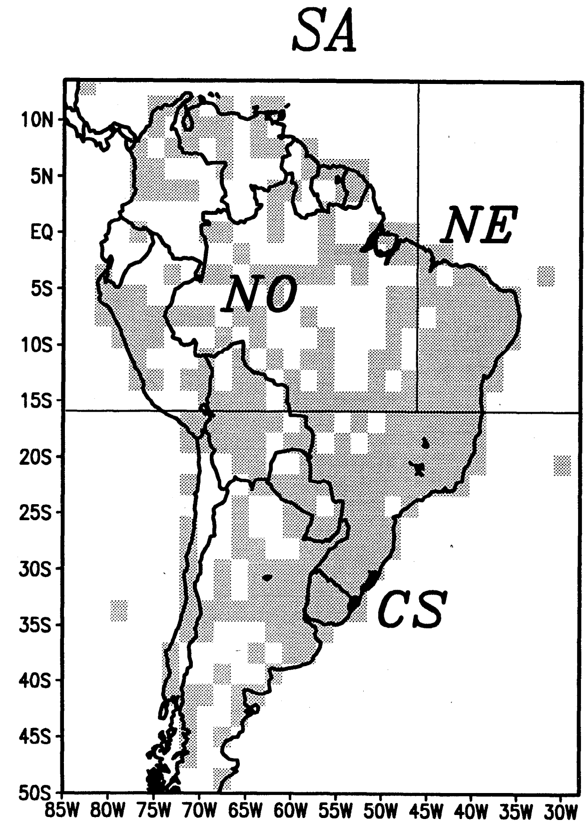

Figure 8. South America (SA) sectors: north (NO), northeast (NE), center-south (CS) where equitable threat score and bias score were estimated. In shaded areas are grid-boxes of 1.875°×1.875° latitude-longitude resolution which contained at least one surface observation in August 1997.

GCM. The temperature gradients are better depicted in the regional model.

In the Amazon region, although there are few observations for doing a reliable comparison, both models show different patterns from observations. While the regional model produces some gradients in the meridional direction, the GCM show some gradients in the zonal direction. A weakness of the regional model may reside in the treatment of water in the soil which is based on the bucket model, where the vegetation formulation is not included. Therefore the temperature field continues to follow the topography pattern. The GCM has the SiB scheme [*Sellers et al.,* 1986] which gives a complex treatment to soil water. This scheme can improve the surface variables for longer-range forecasts. However, at T62 truncation, the topography exhibits strong undulations due to Gibbs effects. As a consequence, the temperature fields follow this undulations, and these propagation is seen in the direction perpendicular to the orientation of the topography.

4.1.4. Threat and bias scores. Only grid points which contained at least one observation were included in the computation of equitable threat score and bias score. owing to the distinct weather regime over different parts of the continent, the scores over South Amer-

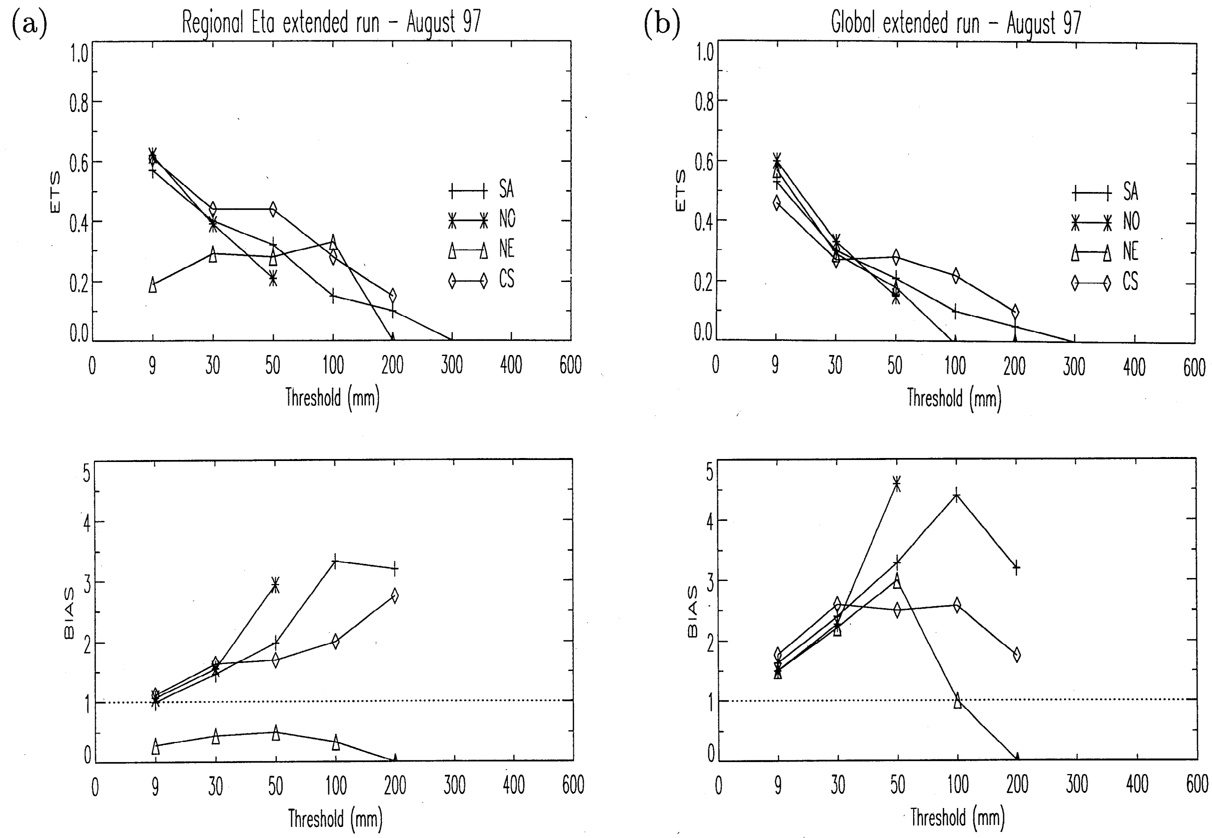

Figure 9. Equitable threat score and bias score for monthly total precipitation predicted by (a) the regional eta model and (b) global model, for August 1997. SA refers to whole South America domain, NO, north; NE, northeast; and CS, center-south regions, as defined in Figure 8.

ica (SA) were divided into three regions: north (NO), northeast (NE) and center-south (CS). These regions are shown in Figure 8. The scores were based on the daily precipitation observation data set received in real time at CPTEC. These observations were summed up into a monthly total precipitation of 651 observation sites over South America. This data set distinguishes from those in Figure 5a, INMET data, by the inclusion of surface automatic weather station and synoptic observations from other countries of South America. The monthly total precipitation data set reported by INMET is restricted to Brazil; however, it includes climatological surface stations which do not report in real time.

The equitable threat score (Figure 9) shows that the regional model produces good forecasts of precipitation at low amounts. For larger amounts, the number of observations are small, and the significance of the result also becomes less reliable. Table 1 shows the number of grid-boxes with observed amounts higher than each threshold. The score drops sharply from the first threshold to the others. The center-south region shows the best score among the three regions. The northeast of Brazil shows the worst score due to the small number of observed precipitation. During this time of the year, precipitation is generally restricted along the eastern coast of northeast Brazil [*Rao et al.*, 1993].

The bias score corroborates part of the results from section 4.1.1. Precipitation values over the northeast of Brazil were underestimated as are indicated with bias values < 1. In the north region (NO), some countries, such as Colombia, reported only a very few number of observations; the total monthly precipitation was therefore smaller than the predicted amounts. These results are indicated by a bias score > 1. Over the center-south region the precipitation at low amounts are well predicted by the regional model; however, at higher amounts the model overestimates. This score may be influenced by the floods produced in the regional model.

Compared to the scores produced by the GCM forecasts (Figure 9b), the regional model shows generally higher scores indicating improvement in the forecasts. The GCM overestimates the forecasts at higher amounts. Over the northeast of Brazil (NE), models show different behavior; while the regional model underestimates the precipitation, the global model overestimates it. The smaller number of rain observations in this period results in a smaller score, as less events are counted.

4.2. Rainy Month Run: November 1997

4.2.1. Precipitation. Rains have resumed over the central part of the continent in the beginning of spring (Figure 10a). The general pattern of the regional

Table 1. Number of Points With Observation Above the Thresholds in August 1997

Regions	Precipitation Thresholds, mm						
	9.	30.	50.	100.	200.	300.	400.
SA	163	84	49	15	5	0	0
NO	70	40	17	0	0	0	0
NE	18	9	6	3	1	0	0
CS	75	35	26	12	4	0	0

model precipitation forecast (Figure 10b) compares reasonably with observations; however, a tendency for drying in the northeast of Brazil still persists in this run. Observed isolated patches of precipitation maxima in the central states of Brazil is missing from the forecasts, although the general amounts over 100 mm were forecast. In November 1997 the El Niño event was well established with warm sea surface temperatures over the Pacific Ocean. During typical El-Niño years, negative anomalies of precipitation are observed over the Amazon [*Marengo*, 1992; *Marengo et al.*, 1998]. The largest amounts in the regional model and in the observations are between 200 and 300 mm, which are close to climatology. The GCM forecast produced in general more rain than the regional model (Figure 10c).

4.2.2. OLR. During the rainy month the main OLR feature (Figure 11a) was the band of low values, below 220 $\mathrm{W m^{-2}}$, associated with a precipitation region above 200 mm, which extended from the Amazon to the southeast of the continent. This band resembles the SACZ although slightly displaced southward. Both, regional and global models overestimated OLR in the domain (Figures 11b and 11c). The OLR band of low values was missed by the regional model; however, the global model captured the southern part of this band which was related to the high precipitation amounts observed over the southeast of Brazil. This suggests that the clouds in the regional model were not active enough to reach higher cloud tops and to produce larger amounts of precipitation.

The minimum values predicted by the global model along the Andes are related to the precipitation maxima over the Cordillera. This model behavior seems to be caused by the topography representation which is based on the sigma vertical coordinate; besides, at a coarser resolution, mountain tops are lower. On a terrain-following coordinate, the horizontal flow can transpose the mountains with less difficulty than the step-orography eta coordinate and easily induce moisture convergence. The minimum of OLR is less evident in August when moisture availability is largely reduced preventing the formation of deep convection. Finally, the comparisons should be restricted to the general patterns, as the observed OLR was derived from once daily satellite passages and different resolutions are used by the models and observations.

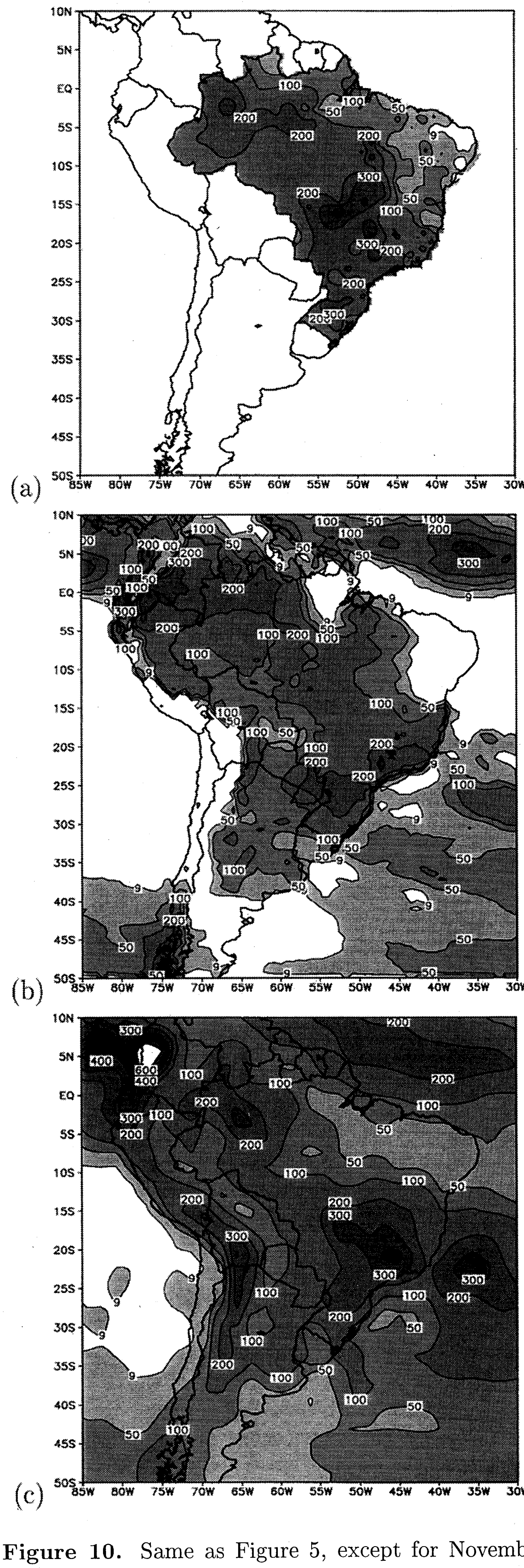

Figure 10. Same as Figure 5, except for November 1997.

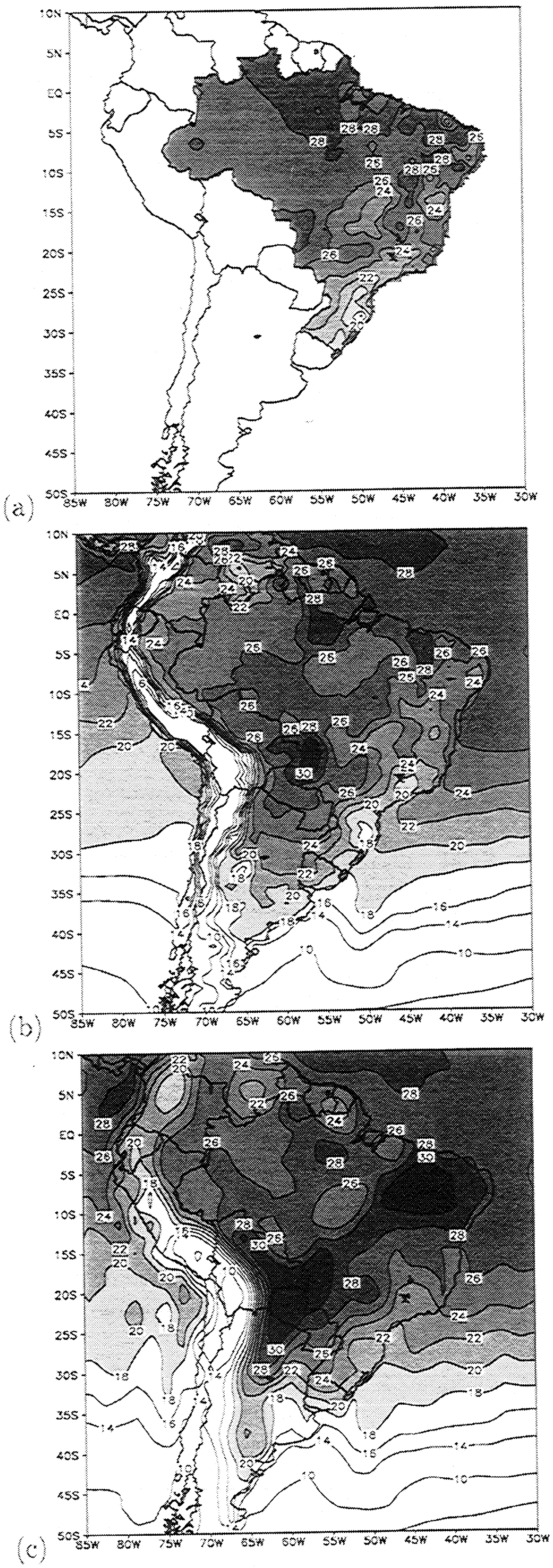

Figure 11. Same as Figure 6, except for November 1997.

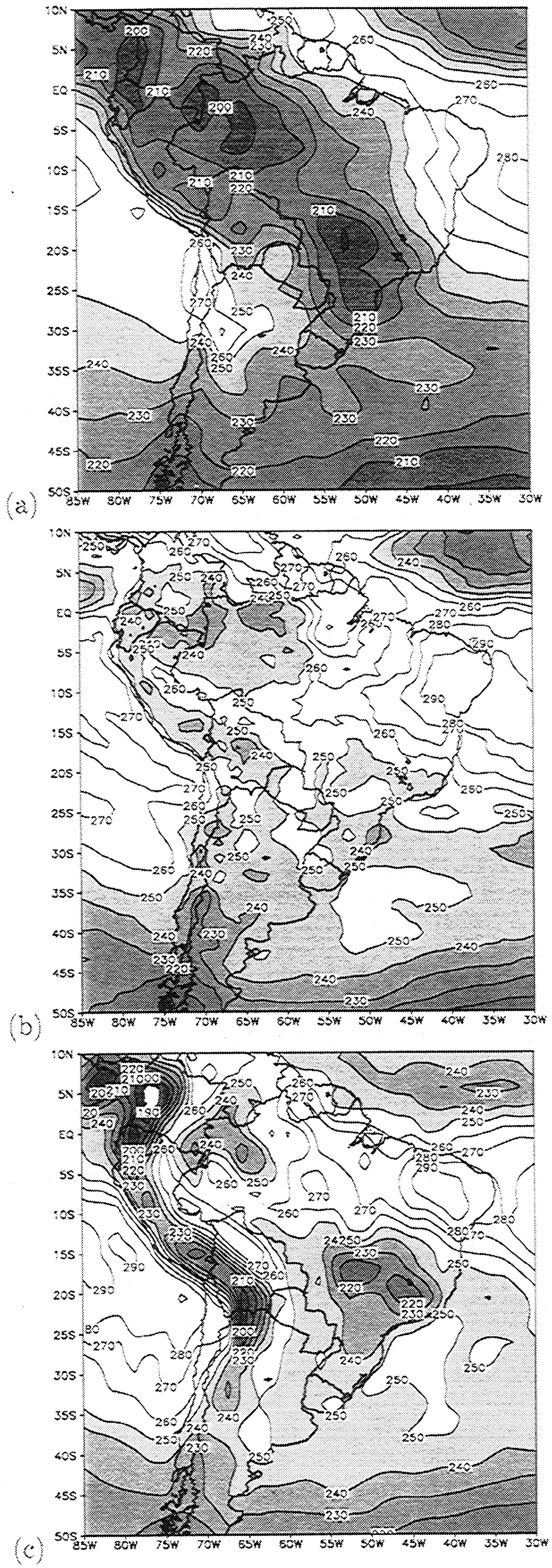

Figure 12. Same as Figure 7, except for November 1997.

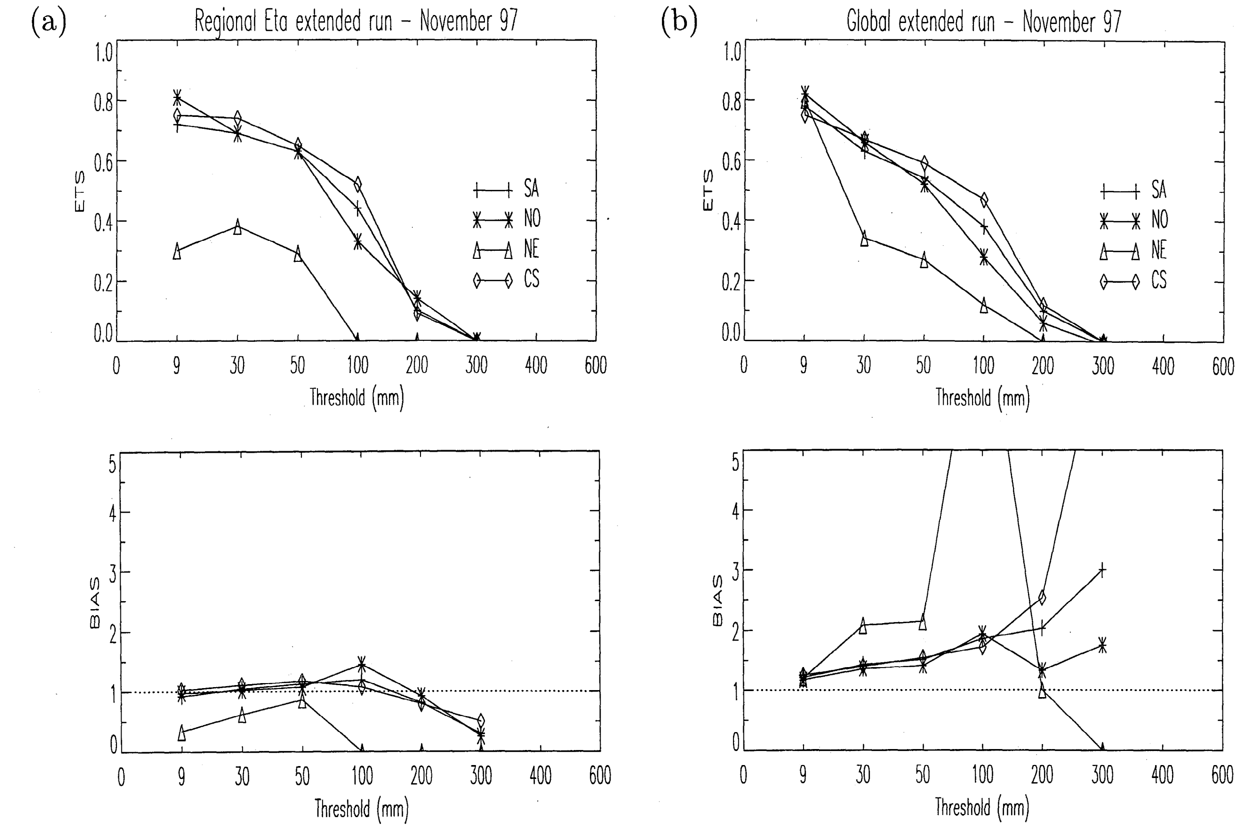

Figure 13. Same as Figure 9, except for November 1997.

4.2.3. Temperature. The regional model forecasts of surface temperature show good agreement with observations (Figure 12). The cold air intrusion along the southeastern coast is detailed in the forecasts; not only the pattern of the contours but also the absolute value of forecast surface temperatures are comparable to observed screen temperature. The global model captures the large-scale patterns, and the details are provided by the regional model. The forecasts seem to be poor again over regions covered by the tropical forest. The observed temperature homogeneity in the Amazon region is poorly forecast by both models, which tend to be slightly colder. However, in the interior of the vast forest regions, the reduced number of observed data impedes a conclusive verification.

4.2.4. Threat and bias scores. Values of equitable threat score ~ 1 (Figure 13a) in the rain/no-rain threshold show that the model captures well the precipitation region; however, the score drops sharply for thresholds of 200 mm. Similar to the dry case, the center-south region produces the largest scores, followed by the north region, and the smallest scores are in the northeast region. During this month the bias score is closer to 1 in the center-south region indicating good forecasts. In the north, precipitation at 100 mm threshold is overestimated. In the northeast, precipitation is underestimated at most thresholds; this is shown with the bias score smaller than 1.

The GCM scores (Figure 13b) are similar to the regional but slightly lower. Differences are noted in the bias score which shows the GCM overestimates precipitation in all regions, mostly over the northeast. Table 2 shows the number of grid points with observations above each threshold for this month.

5. Discussion and Conclusions

Extended runs of 1-month length period were carried out with the regional eta model over South America. These runs were performed for a dry and a rainy month of South America regime in order to evaluate the model ability to produce regional climate forecasts for this continent.

The regional eta model proved to be able to produce 1 month climate prediction for South America. The re-

Table 2. Number of Points With Observation Above the Thresholds in November 1997

Regions	Precipitation Thresholds, mm						
	9.	30.	50.	100.	200.	300.	400.
SA	247	197	165	95	32	7	0
NO	96	81	69	33	12	4	0
NE	30	13	7	1	1	1	0
CS	121	103	89	61	19	2	0

sults were compared to the GCM forecasts in order to evaluate the positive contribution of the regional runs. The regional forecasts showed that the higher resolution could provide more detail to the forecasts, particularly for the temperature. The magnitude of predicted variables was in general closer to observations. It should be reminded that part of the quality of regional forecasts have some dependence on the quality of the global model forecasts.

The improvement on the forecast with the regional model was more significant during the dry month. This shows the model usefulness to predict low temperatures related to the frequent cold air outbreaks during the winter season, which largely affect the coffee-growing areas of Brazil. During the wet month the regional model underestimated the precipitation and overestimated OLR over the central part of Brazil. This result can suggest a deficiency in the model convective scheme in producing more active deep clouds. The simplicity of the land surface scheme may also play part in the model deficiency during the wet month. Forecasts over the tropical forest region are sensitive to both schemes. An improved treatment of water transports in the soil and atmosphere can presumably produce improved long-term forecasts with the eta model over South America. The inclusion of a more sophisticated land-surface scheme is being tested.

SST was kept constant during the integration of both models, regional and global. The large or sudden change in the SST anomalies cannot be followed by the models. During the wet month, November 1997, the negative SST anomalies along the southeastern coast of South America shifted to high positive anomalies.

Owing to the high nonlinearity of the model, integrations based on the use of different initial conditions and/or different model physics are being considered for these extended range forecasts. The ensemble technique could give confidence to these results and improve them. Nevertheless, in the present work, the forecasts produced by the regional model still indicate the suitability of the current configuration for 1-month continuous integrations and the positive contribution over the GCM.

Acknowledgments. The authors would like to thank the two anonymous reviewers for their comments to help clarify the paper.

References

Bell, G. D., and M. S. Halpert, Climate assessment for 1997, *Bull. Am. Meteorol. Soc., 79*, S1-S50, 1998.

Betts, A. K., and M. Miller, A new convective adjustment scheme, Part II, Single column model tests using GATE wave, Bomex and arctic air-mass data sets, *Q. J. R. Meteorol. Soc., 112*, 693-709, 1986.

Black, T. L., The new NMC Mesoscale Eta Model: Description and forecast examples. *Weather Forecasting, 9*, 265-278, 1994.

Bonatti, J. P., J. L. Gomes, S. C. Chou, and A. M. B. Nunes, Nesting of numerical models for severe storm forecast (in Portuguese), paper presented at IX Congresso Brasileiro de Meteorologia, Campos do Jordão, SP, Brazil, Soc. Bras. de Meteorol., Dep. de Meteorol., Rio de Janeiro, 1996.

Cavalcanti, I. F. A, P. Nobre, M. L. Abreu, M. Quadro, and L. P. Pezzi, Vertical and horizontal resolution comparisons of CPTEC/COLA GCM, paper presented at Twentieth Annual Climate Diagnostics Workshop, Seattle, Washington, National Oceanic and Atmospheric Administration, Oct. 23-27, 1995.

Chou, S. C., and M. G. A. Justi da Silva, Evaluation of the eta model precipitation forecasts over South America, in *Climanálise*, vol. 14, Instituto Nacional de Pesquisas Espaciais, Cachoeira Paulista, Brazil, 1999.

Dacić, M., Regional climate modeling using eta model: Mediterranean simulation preliminary results. paper presented at International Symposium on Cyclones and Hazardous Weather in the Mediterranean, World Meteorological Organization, Palma de Mallorca, Spain, 1997.

Davies, R., Documentation of the solar radiation parameterization in the GLAS climate models, *NASA Tech. Memo., 83961*, 57 pp., 1982.

Dickinson, R. E., R. M. Errico, F. Giorgi, and G. T. Bates, A regional climate model for the Western United States, *Clim. Change, 15*, 383-422, 1989.

Giorgi, F., and G. T. Bates, The climatological skill of a regional model over complex terrain, *Mon. Weather Rev., 117*, 2325-2347, 1989.

Giorgi, F., and L. O. Mearns, Introduction to special section: Regional climate modeling revisited, *J. Geophys. Res., 104*, 6335-6352, 1999.

Giorgi, F., M. R. Marinucci, and G. T. Bates, Development of a second-generation Regional Climate Model (RegCM2), Part I, Boundary-layer and radiative transfer processes, *Mon. Weather Rev., 121*, 2794-2813, 1993.

Harshvardhan, R. D., D. A. Randall, T. G. Corsetti, A fast radiation parameterization for general circulation models, *J. Geophys. Res., 92*, 1009-1016, 1987.

Janjić, Z. I., Forward-backward scheme modified to prevent two-grid-interval noise and its application in sigma coordinate models, *Contrib. Atmos. Phys., 52*, 69-84, 1979.

Janjić, Z. I., Nonlinear advection schemes and energy cascade on semi-staggered grids, *Mon. Weather Rev., 112*, 1234-1245, 1984.

Janjić, Z. I., The step-mountain coordinate: Physical package, *Mon. Weather Rev., 118*, 1429-1443, 1990.

Janjić, Z. I., The step-mountain coordinate: Further developments of the convection, viscous sub-layer, and turbulence closure schemes, *Mon. Weather Rev., 122*, 927-945, 1994.

Ji, Y., and A. D. Vernekar, Simulation of the Asian summer monsoons of 1987 and 1988 with a regional model nested in a global GCM, *J. Clim., 10*, 1965-1979, 1997.

Kinter, J. L., III, J. Shukla, L. Marx, and E. Schneider, A simulation of the winter and the summer circulations with the NMC global spectral model, *J. Atmos. Sci., 45*, 2486-2522, 1988.

Kinter, J. L., III, D. DeWitt, P. A. Dirmeyer, M. J. Fennessy, B. P. Kirtman, L. Marx, E. K. Schneider, J. Shukla, and D. Straus, The COLA atmosphere-biosphere general circulation model: Formulation, *Tech. Rep., 51*, vol. 1, 46 pp., Cent. for Ocean-Land-Atmos. Stud., Calverton, 1997.

Kuo, H. L., Further studies of the parameterization of the influence of cumulus convection on large scale flow, *J. Atmos. Sci., 31*, 1232-1240, 1974.

Lacis, A. A., and J. E. Hansen, A parameterization of the absorption of solar radiation in the earth's atmosphere, *J. Atmos. Sci., 31*, 118-133, 1974.

Liebmann, B., and C. A. Smith, Description of a complete (interpolated) outgoing longwave radiation dataset, *Bull. Am. Meteorol. Soc., 77*, 1275-1277, 1996.

Liu, Y., F. Giorgi, and W. M. Washington, Simulation of summer monsoon climate over East Asia with an NCAR Regional Climate Model, *Mon. Weather Rev., 122*, 2331-2348, 1994.

Manabe, S., Climate and the ocean circulation, 1, The atmospheric circulation and the hydrology of the earth's surface, *Mon. Weather Rev., 97*, 739-774, 1969.

Marengo, J., Interannual variability of surface climate in the Amazon basin, *Int. J. Climatol., 12*, 853-863, 1992.

Marengo, J., J. Tomasella, and C. Uvo, Long-term streamflow and rainfall fluctuations in tropical South America: Amazonia, Eastern Brazil and Northwest Peru, *J. Geophys. Res., 103*, 1775-1783, 1998.

Mellor, G. L., and T. Yamada, A hierarchy of turbulence closure models for planetary boundary layers, *J. Atmos. Sci., 31*, 1791-1806, 1974.

Mellor, G. L., and T. Yamada, Development of a turbulence closure model for geophysical fluid problems, *Rev. Geophys., 20*, 851-875, 1982.

Mesinger, F., A blocking technique for representation of mountains in atmospheric models, *Riv. Meteorol. Aeronaut., 44*, 195-202, 1984.

Mesinger, F., and T. Black, On the impact on forecast accuracy of the step-mountain (eta) vs. sigma coordinate, *Meteorol. Atmos. Phys., 50*, 47-60, 1992.

Rao, V. B., M. Lima, and S. H. Franchito, Seasonal and interannual variations of rainfall over Eastern Northeast Brazil, *J. Clim., 6*, 1754-1763, 1992.

Sass, B. H., and J. H. Christensen, A simple framework for testing the quality of atmospheric limited area models, *Mon. Weather Rev., 123*, 444-459, 1995.

Sellers, P. J., Y. Mintz, Y. C. Sud, A. Dalcher, A simple biosphere model (SiB) for use within general circulation models, *J. Atmos. Sci., 43*, 505-531, 1986.

Souza, E. B., J. M. B. Alves, and C. A. Repelli, A mesoscale convective complex associated with intense precipitation over Fortaleza-CE (in Portuguese), *Rev. Bras. Meteorol., 2*, 1-14, 1998.

Tanajura, C. A. S., Modeling and analysis of the South American summer climate, Ph.D. thesis, 164 pp., University of Md., College Park, 1996.

Tiedtke, M., The sensitivity of the time mean large scale flow to cumulus convection in the ECMWF model, paper presented at Workshop on Convection in Large Scale Numerical Models, Eur. Cent. for Medium-Range Weather Forecasts, Reading, England, 1983.

Xue, Y., P. J. Sellers, J. L. Kinter III, and J. Shukla, A simplified biosphere model for global climate studies, *J. Clim., 4*, 345-364, 1991.

I. F. A. Cavalcanti, S. C. Chou, and A. M. B. Nunes, Centro de Previsão de Tempo e Estudos Climáticos - CPTEC, Instituto Nacional de Pesquisas Espaciais - INPE, Cachoeira Paulista, 12630-000 SP Brazil. (iracema@cptec.inpe.br; chou@cptec.inpe.br; bueam@cptec.inpe.br)

(Received April 13, 1999; revised October 28, 1999; accepted November 10, 1999.)